GMR
The Original

CARDIOVASCULAR RISK IN PATIENTS WITH TAKAYASU ARTERISTIS USING DEEP GATED ATTENTION BAG LEVEL CLASSIFIER

Reshma S.Ravi [1], K. Vanitha[2]

[1]Research Scholar Department of Computer Science and Engineering KAHE Coimbatore, India reshmasravi@gmail.com
[2]Associate Professor Department of Computer Science and Engineering KAHE Coimbatore, India
vanitha.krishnan@kahedu.edu.in
Corresponding Author: Reshma S.Ravi*

Abstract
Takayasu Arteritis (TA) being a chronic inflammatory state chiefly influences the aorta and its crucial branches, resulting in severe Cardio Vascular Disease (CVD) impediments. TA-CVD detection employing image analysis is more complex and hence to design a Deep Learning based computer aided solution is indispensable to address this demanding issue. To focus on this issue, a Gated Attention Bag Level Classifier (GA-BLC) design that can automatically extract representative features from TA images for identifying cardiovascular risk in patients. GA-BLC method consists of three stages, pre-processing using Deep Learning Reconstruction Weighted Contrast-enhanced Pre-processing model, CutMixaugmentationandResNet Gated Attention Bag-level Classifier for Cardiovascular Prediction in Patients with Takayasu Arteristis. To evaluate the performance of obtained deep features, bag-level classifier is applied. The experimental results for clinical data with TA along with training images show that the deep features with bag-level classifier achieve the highest performances 13% accuracy and 25% accuracy compared to the conventional classifier. Moreover the inter-reliability and intra-reliability were found to be improved by 14% and 18% compared to the traditional classifier. The findings put forward that our proposed method has competence to locate biomarkers for diagnosis of cardiovascular risk in patients with TA, which will aid in the evolution of computer assisted diagnostic method by specialists.

Keywords: Takayasu Arteritis, Computed Tomography Angiography, CutMix augmentation, Deep Multiple Instance Learning, Bag-level classifier.

1. Introduction

Diagnosing Takayasu Arteritis (TA) necessitates discerning its heterogeneous indicators like fatigue, fever and pulse differences, then utilizing sophisticated imaging like CT Angiography (CTA)or MR Angiography (MRA) scans to visualize inflammation and blockages in the aorta and its branches, supported by blood tests for inflammation markers and clinical criteria (i.e. The American College of Rheumatology) to confirm the diagnosis. In [1], Deep Learning Reconstruction with Dark Blood (DLR-DB) was proposed with the intent of improve quality of image for CTA. Here by applying deep learning reconstruction technique presented higher quality and subjective scores therefore improving the signal to noise ratio (SNR). With this design of combining dark blood with deep-learning reconstruction resulted in the best overall performance.Despite improvements observed in terms of SNR, however the precision and accuracy factors were not focused.

In [2] with the intent of predicting risk involved in stroke and myocardial infarction in Takayasu arteritis using automated machine learning models. Here, eXtreme Gradient Boosting (XGBoost) automated machine learning models was applied to focus on the accuracy aspect of high-risk patients. In spite of the major concentration on the accuracy aspects of high-risk patients being governed, however the false positive rate and false negative rate were not concentrated. In [3] identification of vulnerability loci for TA by means of conducting extensive multi-ancestral genome-wide association study was presented that in turn provided guidelines for new therapeutic targets. Both Ultrasound and MRI are put forward as first line diagnostic test in TA however local expertise and potential diagnoses are paramount for imaging modality selection. The advantages and drawbacks of applying TA, its applications in diagnosis and management were discussed in detail in [4].

Takayasu arteritis (TAK) is a rare vasculitis specifically influencing the aorta and its branches. The insufficiency of Aortic valve (AV) is a clinically notable but unfamiliar representation of TAK. A patient cohort analysis using dark blood T2 weighted mechanism was applied in [5] to minimize the scan time. Yet another

reconstructive algorithm [6], employing deep learning (DL) was proposed to ensure improved tissue differentiation with better image quality. Nevertheless early diagnosis was focused in [7] via multidisciplinary management and its impact on long-term outcomes.

Takayasu arteritis as stated earlier an infrequent inflammatory disease that chiefly takes hold off medium- and large-sized arteries, specifically the aorta and its branches. In [8], an algorithm was designed with the objective of measuring the quality of image employing novel dark-blood computed tomography angiography (CTA) imaging with deep learning reconstruction (DLR). This method was designed in order to visualize cervical artery wall in patients with TAK with high diagnostic confidence level. Yet another image reconstruction algorithm employing DL was proposed in [9] to not only reduce image noise but also to image quality involved. A comprehensive review of cerebrovascular influences on TA was investigated in [10]. A systematic review and more precise estimate of the pooled pervasiveness of each angiographic type was investigated in [11] using clinical Manifestations.

Clinical evaluation of TA patients is demanding owing to disease activity is both laborious and cumbersome to define and measure. Historically, both medical history and physical examination have been the understructure to measure disease activity in TA. Nevertheless, precisely differentiating between normal and diseased can be difficult at the bedside. To optimize and harmonize the follow-up of TA French recommendations were included in [12]. Disease activity index were measured in [13] to assess the performance within standpoint observational cohort of patients with TA. However analysis was not made for clinical features. To focus on this aspect, diagnostic procedures and TA management in longitudinal cohort of patients within a single region of southern Italy was detailed in [14]. A case-control study to observe delayed contrast-enhanced MRI in patients with TA MRA was presented in [15]. Inferences were also made that declared free breathing could access TA to be one of the chief characteristics.

One of the significant health concerns faced over the recent few years is Cardio Vascular Disease (CVD). Timely and accurate identification of CVD remains a major issue to be handled by the healthcare systems globally. There arises a requirement of novel technical mechanisms for ensuring accurate and precise TA-CVD identification. In this research GA-BLC based on a representative feature extraction model along with bag-level classifier is proposed.

1.1 Contributions of the paper

To address on the above said issues, like handling false positive rate and false negative rate with focus on accurate disease detection results using the images and clinical data of TA, a method called, Gated Attention Bag Level Classifier (GA-BLC) for analyzing cardiovascular risk in patients with TA is designed. The contributions of the GA-BLC are listed as given below.

- To design a robust analysis of cardiovascular risk in patients with TA method, GA-BLC is designed based on pre-processing, feature extraction and classification.
- To improve sensitivity and accuracy for the detection and assessmentby reducing noise ensuring better image quality Deep Learning Reconstruction Weighted Contrast-enhanced Pre-processing model is applied.
- To design ResNet Gated Attention and Deep Bag-level Classifier for Cardiovascular Prediction in Patients with Takayasu Arteristis that by applying Discrete Instance Learning rather than a single instance aids in improving the overall precision and recall. Also by applying DL based ResNet Feature Extractor extracts meaningful features automatically therefore minimizing false positive and false negative rate.
- To improve accuracy along with the intra-reliability and inter-reliability by applying Bag-level Classification for measuring cardiovascular risk in patients with TA in a significant manner.
- Finally, complete experimental evaluation is performed with five different performance metrics, precision, recall, accuracy, false positive rate and false negative rate to illustrate the proposed GA-BLCmethod over traditional methods.

1.2 Organization of the work

This paper is organized as follows: In Section 2, we motivate our study by setting in motion the background and related work involving risk analysis of cardiovascular in patients with TA using deep learning techniques. In Section 3, we present the details of our proposed Gated Attention Bag Level Classifier (GA-BLC) method for efficient disease diagnosis. A detailed case study applying images and clinical data is presented in Section 4 ensuring qualitative analysis. Experimental results along with a comprehensive discussion with conventional methods with the aid of table and graphical representations are included in Section 5. Finally, concluding remark is included in Section 6.

2. Related works

As a consequence of reasonable morbidity and mortality, precise and time diagnosis plays a pivotal role in boosting the outcomes for patients with TA. Woefully, the ambiguous clinical presentations and laboratory test outcomes commonly accord to late diagnosis and hamper treatment. Pulmonary artery lesions in TA employed delayed contrast enhanced MI was proposed in [16]. With this type of design boosted the effectiveness of evaluating status of disease. Yet another method was presented in [17] to utilize coronary CR angiography to distinguish involvement of artery in patients with known TA with shortness of breath. The results confirmed that most coronary lesions were found in proximal coronary artery locations.

Imaging tools are found to be well established diagnostic tests while imparting significant information concerning vascular damage occurrence. A review strives to impart the current status of multimodality imaging for diagnosis in the area of large vessel vasculitis was presented in [18]. In accordance with the arteries involvement, six types of Takayasu arteritis are reported in [19] with the objective to demonstrate the several multidetector CT angiography appearances of TA and to discuss in detail different diagnosis mechanisms. In [20] a detailed analysis of TA activity assessment to measure flow velocity within the arterial wall was presented.

TA diagnosis is based on heterogeneous factors, to name a few being, incorporation of biological, clinical, demographic and also imaging data. However, the diagnostic value of each clinical indicator remains unclear. An expeditious review and meta-analysis to assess the diagnostic accuracy with precision for clinical signs was presented in [21].Whilst no symptoms of cerebrovascular occurrences are found during recent evaluation of patients with TA, follow-up vascular imaging is paramount for disease progression monitoring and changes in the cerebrovascular risk.

Nevertheless, an optimal imaging algorithm for TA monitoring has not been accepted. A review describing traditional monitoring patterns with novel imaging modalities were discussed in [22]. However the relapse rates were not focused. To address on this aspect, a holistic review and meta-analysis was performed in [23]. A comprehensive review on accurate and early diagnosis of TA was conducted in [24] to reduce psychological burdens.

A deep learning based algorithm including imaging diagnostic framework was designed in [25]. A novel mechanism for TA using MRI for defining disease activity was presented in [26] with improved precision and accuracy. In spite of PET imaging providing high sensitivity in detecting TA, its dependence on visual analysis is hindered by biases. Convolutional neural networks (CNNs) were applied in [27] for enabling automated imaging feature extraction and issues related to segmentation with improved accuracy. The table given below imparts an encapsulation note on most pertinent recent evolutions on unified data representation.

Table 2 Literature representation

S. No	Title	Methods/ Technique	Proposal contribution	Merits	Demerits
1	Large vessel vasculitis evaluation by CTA	Deep Learning Reconstruction with Dark Blood (DLR-DB)	Improve image quality	Higher quality and subjective scores therefore improving the signal to noise ratio (SNR)	Did not focus on accuracy and precision
2	Predicting stroke and myocardial infarction risk in Takayasu arteritis with automated machine learning models	eXtreme Gradient Boosting (XGBoost)	Predicting risk involved in stroke and myocardial infarction in TA	Focus on the accuracy aspect of high-risk patients	Did not focus on false positive rate and false negative rate
3	Identification of susceptibility loci for Takayasu arteritis	Genome wise association study	Identification of vulnerability loci for TA	Improved first line diagnostic accuracy	Focused on local expertise by compromising global aspects
4	Update in imaging for large vessel vasculitis	Machine Learning	Diagnosis of TA	Improved TA diagnostic accuracy	Lack computational complexity

5	Dark blood T2-weighted imaging for tA	Dark blood T2-weighted imaging	Patient cohort analysis for TA	Minimize scan time	Did not concentrate on precision and accuracy factors
6	Deep learning–based reconstruction	Deep Learning based Reconstruction	Tissue differentiation with better image quality	Improved accuracy	Early diagnosis was not focused
7	Long term outcomes of aortic valve insufficiency in patients with TA	Deep Neural Learning	Early diagnosis of TA	Focused on long term outcomes	Image quality was compromised
8	Dark-Blood Computed Tomography Angiography Combined With Deep Learning Reconstruction in TA	Deep Learning Reconstruction	TA diagnosis with quality improved image	High diagnostic confidence level	Image noise were not analyzed
9	Deep Learning Image Reconstruction with TA	DLIR algorithm	Quality improved TA diagnosis	Improved signal to noise ratio	Did not focused on accuracy
10	French recommendations for the management of TA	French recommendations	Precisely differentiating between normal and diseased	Improved precision level	Misclassification was not focused

Motivated by the above literature studies, where certain works focused on precision and accuracy aspects whereas the other concentrated on the false positive rate, in this work a robust Cardiovascular Prediction in Patients with TA called Gated Attention Bag Level Classifier (GA-BLC) is provided in the following sub-sections.

2.1 Research gap analysis

- The main objective of Takayasu Arteritis analysis using deep learning techniques remains in separately obtaining visualizing prominent features like edema, a key indicator of active arteritis formation to ensure robust classification and minimize the risk of falsification of samples thus improving precision and accuracy.
- Using Deep Learning Reconstruction with Dark Blood (DLR-DB) [1] though improved the signal to noise ratio (SNR) for intelligent diagnosis with reconstruction function, however, lack for precise and accuracy results.
- Deep Learning Reconstruction with Dark Blood [1] used limited methods, lacking qualitative perspectives.
- The main emphasis of Deep Learning Reconstruction with Dark Blood [1] remained in improving image quality with little focus on diagnosis.
- eXtreme Gradient Boosting (XGBoost) [2] though with the aid of automated machine learning based prediction boost the effectiveness of clinical diagnosis with improved accuracy however risk of the falsification of images in terms of false positive and false negative rate were not much focused.
- Analysis in eXtreme Gradient Boosting (XGBoost) [2] were made only with high-risk patients

3. Materials and Methodology

3.1 Data Collection and Description

The proposed method for Cardiovascular Prediction in Patients with Takayasu Arteristis in our work uses both clinical data and Magnetic Resonance Angiography (MRA) sample images. The clinical data for the proposed method Takayasu's Arteritis Disease Detection is extracted from

https://data.mendeley.com/datasets/3cfj465shk/1[28]. The clinical data obtained from the dataset consists of 57 patients. The female:male ratio selected for analysis was 4.2:1 with median age at diagnosis to be 29 years. From it, 61.4% of the patients were Caucasians whereas and 86% of the patients had stenosis on imaging. In case of 43.9% vascular interventions were required. Moreover, the most frequent complications were observed to be hypertension with an overall of 56.1%, renal artery stenosis consisting of 28.1% and aortic insufficiency identified to be 19.3% respectively.Moreover MRA samples were obtained from [29] and [30] and using it Cardiovascular Prediction in Patients with Takayasu Arteristis was made in a significant manner.

3.2 Methodology

The key salient feature of the deep learning method is to extract features in an automatic fashion that has advantage for large volume data. In the pre-processing model though with the application of DLR-DB [1] that improved image quality by reducing noise, however in the proposed method using Deep Learning Reconstruction Weighted Contrast Enhanced function with the aid of Dark Blood T2 Weighted aids in improving the overall inter-reliability and intra-reliability. The proposed Gated Attention Bag Level Classifier (GA-BLC) consists of four steps as shown in figure 1.

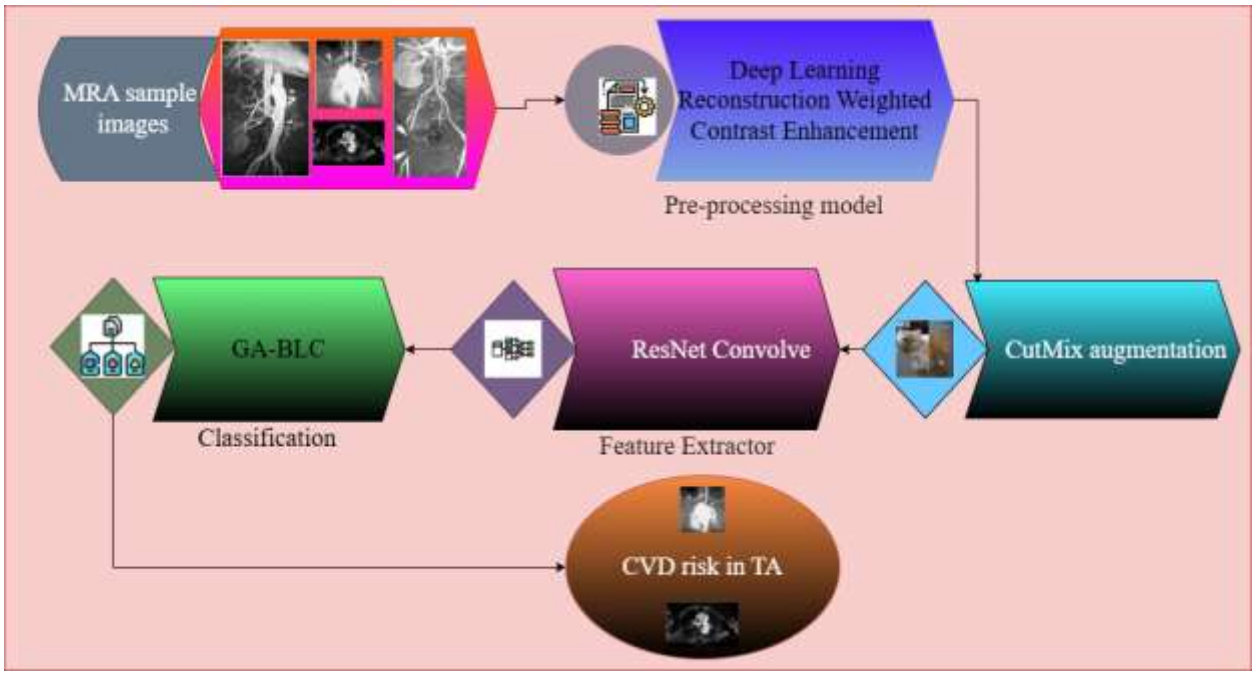

Figure 1 Architecture of the proposed GA-BLC **method**

As shown in the above figure, the overall method is split by performing image pre-processing using training images, augmenting the training time, extracted of prominent features from augmented samples and classification of TA. The first step involves with the training image pre-processing where the contrast is enhanced using the Deep Learning Reconstruction Weighted Contrast Enhanced Pre-processing model. In the second step augmentation of training image is performed by applying the CutMix function. The purpose of using this augmentation is due to the constrained nature of TA image availability for assessing cardiovascular risk. The third step comprises the discrete instance learning followed by feature extraction where the hidden concealed patterns are extracted from augmented samples using the ResNet Gated Attention and Deep Bag-level Classifier for Cardiovascular Prediction in Patients with Takayasu Arteristis. Finally bag-level classifier is applied to classify to prediction Patients with TA. The detail description of the three steps is provided below.

3.2.1 Deep Learning Reconstruction Weighted Contrast-enhanced Pre-processing model

Image pre-processing for Takayasu arteritis (TA) in Magnetic Resonance Angiography (MRA) in our work involves in managing noise and eases accurate quantitative analysis of the vessel. By applying pre-processing techniques assists in visualizing prominent features like edema, a key indicator of active arteritis formation. The sample images obtained from Takaysuarteristisis subjected to cardiovascular monitoring with the aid of Deep Learning Reconstruction magingaids in enhancing image quality by reducing noise and improved visualization of inflamed

arterial walls by means of Dark Blood T2 Weighted function. Figure 2 shows the structure of Deep Learning Reconstruction Weighted Contrast-enhanced Pre-processing model.

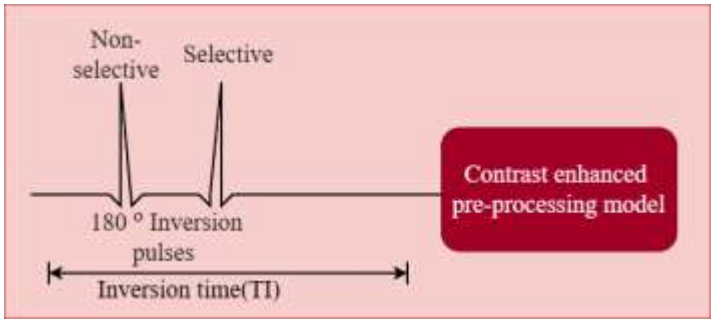

Figure 2 Structure of Deep Learning Reconstruction Weighted Contrast-enhanced Pre-processing **model**

As shown in the above figure, double inversion recovery via deep learning reconstruction function is applied that by using two inversion pulses i.e., non-selective (inverting everything) and selective (inverting only tissue within imaging slice) and hence appears dark. This in turn ensures tissue contrast owing to the reason that normal heart muscle and scar tissue possess shorter T2 time, therefore highlighting areas of scar tissue therefore providing high-quality for diagnosing Takayasu arteristis leading to severe cardiovascular issues. To obtain the contrast enhanced image using the Deep Learning reconstruction functionality via the Signal Intensity Ratio employing Signal Intensity of the Area (i.e. aorta) and Signal Intensity of the Muscle (i.e. left erector spinae muscle) employing Deep Learning Reconstruction Weighted Contrast Enhanced is measured isolated noise components are eliminated. The Signal Intensity Ratio is mathematically formulated as given below.

$$SI_{ratio} = \frac{SI_A}{SI_M} \quad (1)$$

From the above equation (1), Signal Intensity Ratio 'SI_{ratio}' result is arrived at by dividing signal intensity of the abnormal value 'SI_A' by signal intensity of a healthy-appearing muscle 'SI_M' with respect to same image slice respectively. Following which Double Inversion Recovery, a type of Black Blood is applied with the objective of visualizing walls of cardiac chambers and blood vessels using two inversion pulses. The two inversion pulses here refer to the spatially non-selective 'SN' and spatially selective 'SS'. The spatially non-selective refers to the first '180°' pulse inverts within the entire sample space and the second '180°' pulse means its influences are constrained to single slice being imaged. The results generated through both 'SN' and 'SS' are stored in 'Res'. Finally the contrast enhanced image results are obtained as given below.

$$CESI_{ratio} = \frac{SI_A - SI_{ARes}}{SI_M - SI_{MRes}} \quad (2)$$

From the above equation (2), where 'SI_A' is the signal intensity of the abnormal value with 'SI_{ARes}' representing the contrast enhanced T1W1 results of abnormal value, 'SI_M' denoting the signal intensity of a healthy-appearing muscle and finally 'SI_{MRes}' representing the contrast enhanced T1W1 results of healthy-appearing muscle respectively.

3.2.2 CutMixAugmentation

Image augmentation for Cardiovascular Prediction in Patients with Takayasu Arteristis (TA) strives to increase dataset size and diversity, preventing overfitting and therefore enhancing generalization capability to real-world variations irrespective of lighting or angles. In this way by generating synthetic but realistic from existing images, robust features can be learnt, resulting in higher accuracy and better sensitivity (fewer false negatives for critical diseases), across diverse patient groups. With TA being a rare disease, due to lack of sufficient training data, deep learning algorithms struggle to generate accurate and precise detection of results. So CutMix augmentation function is applied to medical images for analyzing conditions like TA. Also by applying the CutMix augmentation function concentrate on manipulating relevant diseased regions rather than random patches. Let '$PS \in \mathbb{R}^{W*H*C}$' and '$Q$' represent a training image and its label and by applying the CutMixaugmentationfunctiontoproduce new training sample '(PS', Q')' by integrating two training samples '(PS_A, Q_A)' and '(PS_B, Q_B)' respectively.Let us define the combining operation as given below.

$$PS' = M \odot PS_A + (1 - M) \odot PS_B \quad (3)$$

$$Q' = \beta Q_A + (1 - \beta) Q_B \quad (4)$$

From the above equations (3) and (4), '$M \in \{0,1\}$' represents binary mask representing the position to drop out and fill in from two images, '1' denoting binary mask filled with ones and '$\odot$' represents multiplication performed element-wise respectively. Moreover the CutMix augmentation function replaces an image region in the training sample with a patch from another training sample therefore generating more locally natural image for further processing. With the objective of sampling binary mask 'M' initially sample bounding box coordinates '$BB = (R_p, R_q, R_w, R_h)$' representing the cropping regions on 'PS_A' and 'PS_B'. The region 'BB' in 'PS_A' is discarded and filled in with patch cropped from 'B' of 'PS_B' respectively. Then, the bounding box coordinates are consistently sampled as given below.

$$R_p = C(0, W), R_w = W\sqrt{1-\beta} \quad (5)$$

$$R_q = C(0, H), R_h = H\sqrt{1-\beta} \quad (6)$$

From the above equations (5) and (6), the binary mask '$M \in \{0,1\}$' is arrived at by padding with '0' within the bounding box 'BB', on contrary '1'. By applying the above function concentrate on fine-drawn, localized diseased features instead of global patterns, therefore improving generalization, resulting in better performance in diagnosing conditions like TA.

3.2.3 ResNet Gated Attention and Deep Bag-level Classifier for Cardiovascular Prediction in Patients with Takayasu Arteristis

Takayasu Arteritis (TA) notably heightens the risk involved in cardiovascular, with clinical predictors for events including older age, hypertension, higher BMI, high inflammatory markers (ESR) at onset and so on along with key MRI findings consisting of vessel wall inflammation, acute myocardial edema, significant occlusion. In our work ResNet Gated Attention and Deep Bag-level Classifier for Cardiovascular Prediction in Patients with Takayasu Arteristisis applied that by utilizing neural networks of deep learning aids in learning the instances (i.e. image patches) that are found to be most important within a bag (i.e. a whole image). Figure 3 shows the structure of ResNet Gated Attention Bag-level Classifier.

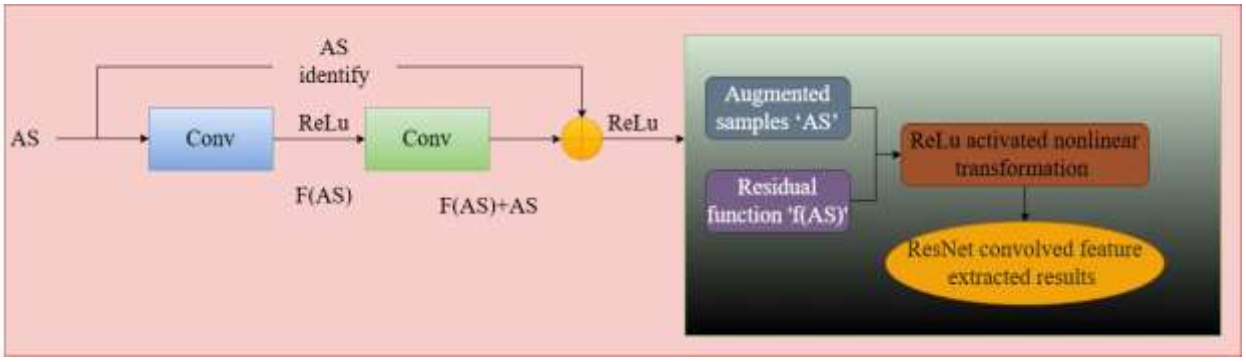

Figure 3 Structure of ResNet Gated Attention Bag-level Classifier

As shown in the above figure, to start with ResNet Gated Attention Bag-level Classifier is formulated. Here, instead of a single class label multiple instance learning via ResNet Gated Attention is assigned to a bag of instances. Next, using a combination of convolutional and fully connected layers via ResNet-based feature extractor, all transformations are parameterized using neural networks and hence is referred to as Discrete instance learning. This in turn boosts the flexibility by allowing train augmented samples in a comprehensive fashion. Finally, ResNetGated Attention Bag-level Classifier for Cardiovascular Prediction in Patients with Takayasu Arteristis is designed. As far as the binary supervised learning problem is concerned one aims at identifying a model that predicts target variable value '$Q \in \{0,1\}$', for a given sample '$AS \in \mathbb{R}^D$'. However, in case of the ResNet Gated Attention Bag-level Classifier rather than a single instance, a bag of instances (i.e. image patches) are said to exist, '$Pat = \{Pat_1, Pat_2, \ldots, Pat_K\}$', that reveal neither dependency nor specific arrangement among each other. Hence, the prediction follows in the assumption that 'k' differ for different bags. Moreover, a single binary label 'Q' is connected with the bag. Additionally, we also assume that discrete labels exist for the instances within a bag, i.e., '$q_1, q_2, \ldots, q_K$' and '$q_K \in \{0,1\}$', for '$k = 1,2, \ldots, K$'.

$$Q = \begin{cases} 0, iff \ \sum_k q_k = 0 \\ 1, otherwise \end{cases} \quad (7)$$

From the above hypothesis (7) it is inferred that the functions output is said to be permutation invariance providing the results no matter the input has been arranged. The above equation is re-formulated in a compact form with the aid of maximum operator as given below.

$$Q = max\{q_k\} \quad (8)$$

Though feature extraction is automated within deep learning however showing what features are extracted and how they are fine-tuned matters significantly.

3.2.3.1 ResNetConvolvedFeature Extractor

This section strives to extract salient important features in a robust manner from augmented samples 'AS' that make certain efficient detection of Cardiovascular Prediction in Patients with Takayasu Arteristis. Conventional hand-crafted feature extractors select features manually that is not only found to be tedious but also unsophisticated. The DL based ResNet Feature Extractor extracts meaningful features automatically from augmented samples 'AS' using less time.Figure 4 shows a sample residual learning model using ResNet Convolved Feature Extractor.

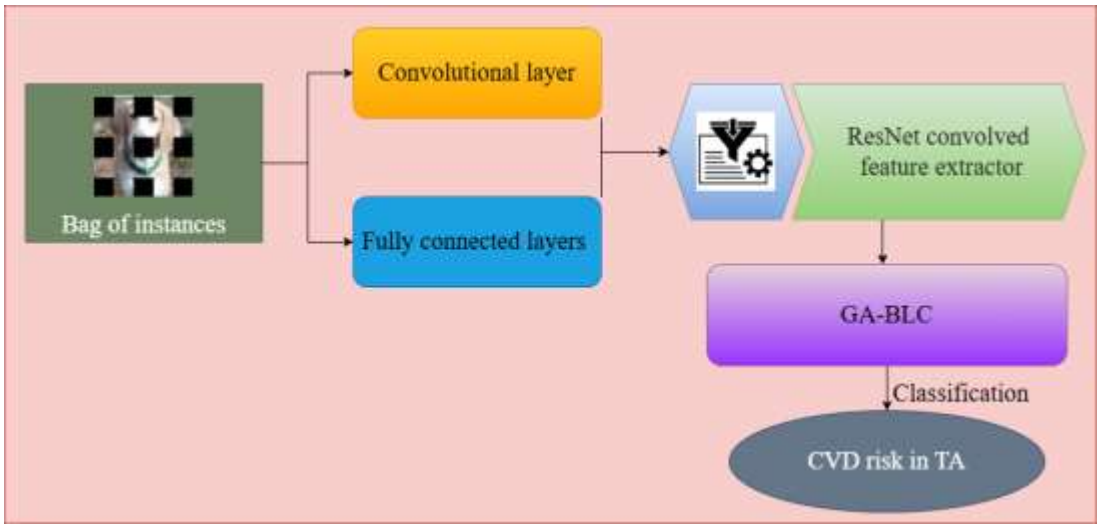

Figure 4 ResNet Convolved Feature Extractor based residual learning model [changes made]

As shown in the above figure, 'AS' is the mapping of input with residual function '$f(AS)$'. Moreover, the ResNet involves with convolutional (Conv) layers, rectified linear units (ReLu) layers that is demonstrated in figure. Moreover, after two divisions (i.e. mapping 'AS' of input and residual function '$f(AS)$') are integrated and are subjected to ReLu activated nonlinear transformation function to create the complete residual learning module result. As shown in the above figure, the input is augmented samples 'AS' and a shortcut is added after 'AS' with the output of the block superimposed upon the input. Hence, the block output is '$f(AS) + AS$' and the network weight parameters require to learn is '$f(AS)$'. Then, finally in the proposed model, residual blocks utilized as basic units of deep ResNet is defined as below.

$$FE = f(AS\{W_i\}) + AS \quad (9)$$

From the above equation (9) the deep sequence of convolutional layers, augmented by residual connections, generates a feature extractor, generating highly informative feature maps for classification process. Also, 'AS' represent input vector and 'FE' represent output vector or the feature extracted results with '$f(AS\{W_i\})$' denoting the residual mapping to be learned.This ResNet Convolved Feature Extractor extracts deep features and then the activation function works on the convoluted results to produce feature map results. The polling layer on the other hand obtains feature from previous layers. Finally, using fully connected layers their outputs (i.e. feature extracted results) are fed to the bag-level classifier for classification task.

3.2.3.2 Bag-level Classifier

Finally in this section a weighted average of patches or low-dimensional embeddings where weights are obtained via neural network called ResNet Gated Attention Bag-level Classifier. Let '$H = \{H_1, H_2, \dots, H_K\}$' denotes the bag of '$K$' embeddings or representing of an individual patch 'Pat_i' within a bag derived by passing patchesvia a function '$H_i = f(Pat_i)$' prior to the aggregation of these sample instance level features '$H_1, H_2, \dots, H_k$' into a single bag for final prediction. Then, the ResNet Gated Attention pooling is represented as given below.

$$z = \sum_{k=1}^{K} Att_k H_k \quad (10)$$

Finally, to perform bag-level classifier ResNetgated attention mechanism is employed and mathematically formulated as given below.

$$Att_k = \frac{exp\{W^T(tanh(Vh_k^T) \odot Sig(Uh_k^T))\}}{\sum_{i=1}^{K} exp\{W^T(tanh(Vh_i^T) \odot Sig(Uh_i^T))\}} \quad (11)$$

From the above equation results (11) tangent '$tanh$' element-wise non-linearity function is used to include both negative and positive values, 'V', 'U' denoting the virtual bag vector representation, U-Net to ensure bag-level classification activated via sigmoid 'Sig' and element-wise multiplication '$\odot$' respectively. On the whole, the proposed ResNet Gated Attention Bag-level Classifier allows assign different weights to instances within a bag. With this the final representation of bag is said to be highly informative for bag-level classifier, therefore ensuring accurate and precise classification results. The pseudo code representation of ResNet Gated Attention Bag-level Classifier for analyzing cardiovascular risk in patients with takayasuarteristis is given below.

Input: Clinical Dataset 'DS', Features '$F = F_1, F_2, \dots, F_n$', Samples '$S = S_1, S_2, \dots, S_m$', Training Images '$P = P_1, P_2, \dots, P_l$'
Output: Robust classified results
Step 1: **Initialize**'$n = 217$', '$m = 57$', '$l = 5$', '$\beta \in [0,1]$' Step 2: **Begin** Step 3: **For** each Clinical Dataset 'DS', Features 'F', Samples 'S' and Training Images 'P' **//Pre-processing** Step 4: Evaluate Signal Intensity Ratio according to (1) Step 5: Generate contrast enhanced image results according to (2) Step 6: **Return** pre-processed samples 'PS' Step 7: **For** each Clinical Dataset 'DS', Features 'F' and pre-processed samples 'PS' **//Data augmentation** Step 8: Define combining operations according to (3) and (4) Step 9: Obtain bounding box coordinate results according to (5) and (6) Step 10: **Return** augmented samples 'AS' Step 11: **For**each Clinical Dataset 'DS', Features 'F' and augmented samples 'AS' **//Discrete Instance creation** Step 12: Formulate discrete instance creation according to (7) and (8) //**ResNet Convolved Feature Extractor** Step 13: Generate feature extracted results according to (9) Step 14: **Return** feature extracted results 'FE' Step 15: **End for** Step 16: **For** each Clinical Dataset 'DS', Features 'F', augmented samples 'AS' and feature extracted results 'FE' Step 17: Generate ResNet Gated Attention pooling results according to (10) and (11) Step 18: **Return** classified results Step 19: **End for** Step 20: **End**

Algorithm ResNet Gated Attention Bag-level Classifier

As given in the above algorithm the entire process of analyzing cardiovascular risk in patients with takayasuarteristis is split into four sections. First, raw training images obtained are subjected to pre-processing employing Deep Learning Reconstruction Weighted Contrast Enhanced Pre-processing. By applying Deep Learning Reconstruction Weighted Contrast Enhanced Pre-processing in our work assists in achieving superior visualization and delineation of myocardial wall and sub-endocardial lesions by hiding the patches from the neighboring bright blood pool. This in turn put forward better sensitivity and accuracy for the detection and assessment compared to traditional methods. Second with Takayasu arteritis being an infrequent disease, making it laborious to gather large, balanced samples for training not only improves generalization by generating more robust features minimizing overfitting but also protect local information within the pasted patches, that is said to be indispensable for detecting fine-drawn vascular wall thickening in medical images. Third the pre-processed and augmented samples are provided as input to the ResNet convolved feature extractor for not only extracting key clinical predictors but also key MRA findings. The main purpose of using this extractor is that it focuses on relevant instances by selectively filtering information in medical imaging, by weighting instance in an adaptive fashion. The ResNetgated attention mechanisms employed here learn

the instances within a bag that are found to be the most important, therefore boosting precision and recall upon compared to simple bag-level pooling. In addition the Discrete Instance Learning employed in our work surpass by integrating deep learning's feature extraction with multiple instance learning to learn from unstructured data like entire slide images by considering patches as instances within a bag. This in turn reduces the false positive and negative rate of detection process. Finally, bag-level classifier with multiple instance learning aids in classifying patients on the basis of the overall pattern of the bag that can assist identify more homogeneous subgroups of the disease than depending on simple scoring systems. Moreover, by grouping samples by their complete disease pattern can provide more accurate information.

Based on the above qualitative results designed for analyzing cardiovascular risk in patients with TA, the quantitative analysis is provided in the following sub-sections.

4. Experimental Setup and Discussion

The proposed Gated Attention Bag Level Classifier (GA-BLC) Cardiovascular Risk in patients with Takayasu Arteristis is evaluated employing Python working on MS Window platform on computer with i3-2350 processor and 2 GB RAM. The results are compared with the previous two existing methods, Deep Learning Reconstruction with Dark Blood (DLR-DB) [1] and eXtreme Gradient Boosting (XGBoost) [2]. The performances of the proposed method isevaluated using practically standard measurements such as precision, recall, accuracy, false positive rate and false negative rate by applying both training images and clinical data.

4.1 Implementation details

In this work to perform simulation analysis of Takayasu Arteritis, a case of a 59-year-old Caucasian woman, with a history of hypertension, thyroid nodules, chronic disease anemia, dyslipidemia, obstructive sleep apnea with use of continuous positive airway pressure, and partially recovered left hemiparesis was used [29] as shown in figure 5.

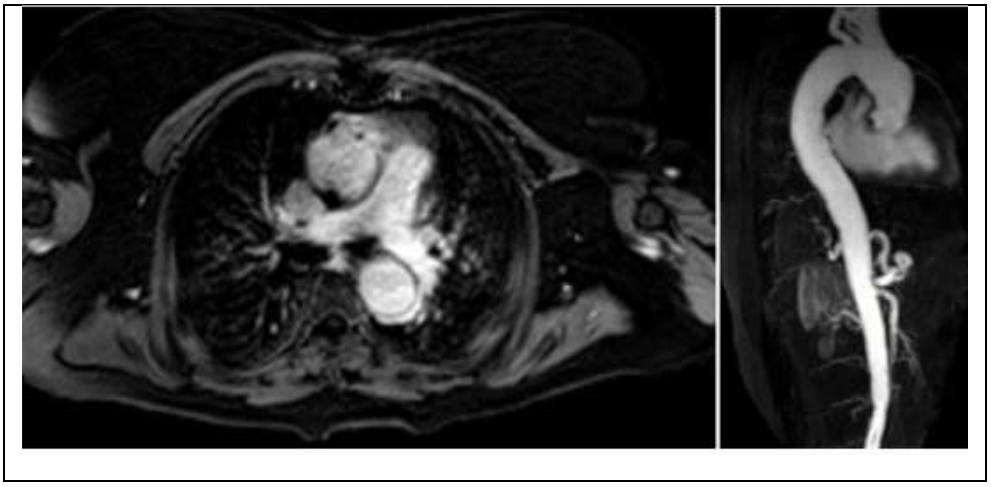

Figure 5 Post-operative MR indicating biological prosthesis correct placement without complications

Findings of TA on MRI include fusiform vascular dilation, thickened arctic valvular cusps [30] and multifocal stenosis as shown in figure 6 given below (a) and (b). Also MR angiography provides detailed vascular information, consisting of the degree, stenoses extent and dilation, location and patency of collateral vessels and surgical bypass grafts as shown in figure given below (c).

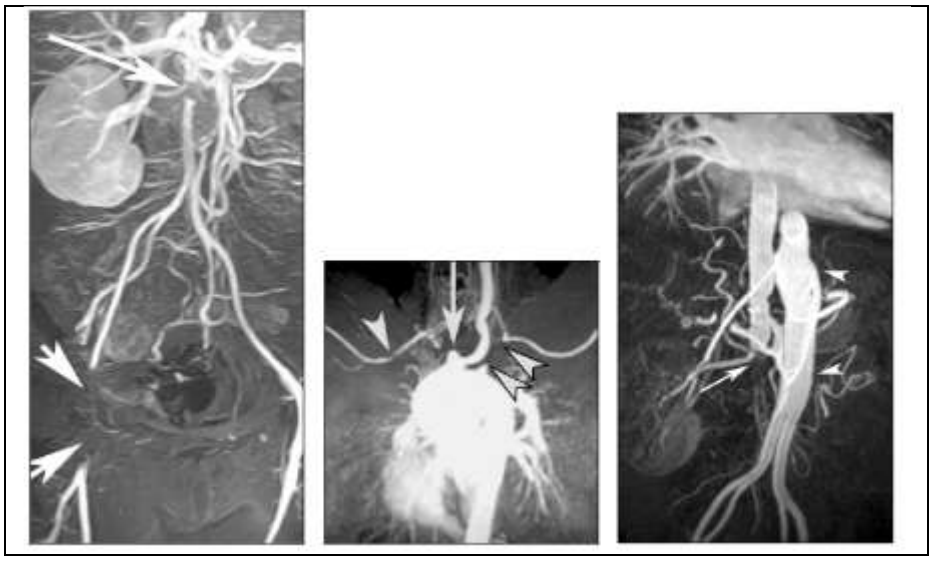

Figure 6(a) 50-year-old woman with Takayasu's arteritis (b) 59-year-old woman with multifocal great vessel stenoses due to Takayasu's arteritis (c) 55-year-old woman with Takayasu's arteritis

With the above sample images provided as input Deep Learning Reconstruction Weighted Contrast Enhanced Pre-processing along with CutMix augmentation is applied to generate the pre-processed and augmented results. These two steps are performed with the intent of improving sensitivity and accuracy for the detection. Figure 7 shows the results of pre-processing and augmentation.

Input images	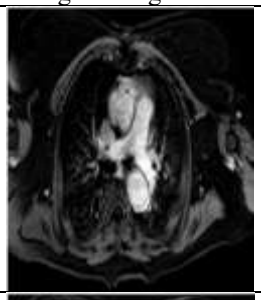	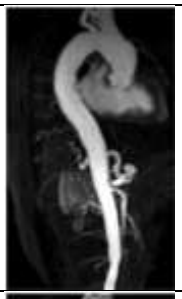	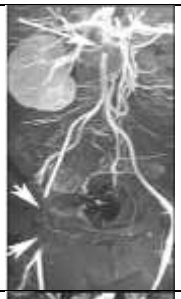	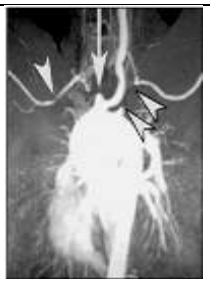	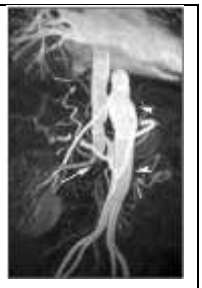
Contrast enhanced images	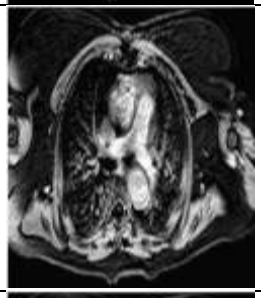	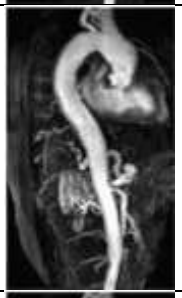	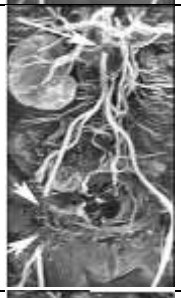		
CutMix Augmented images	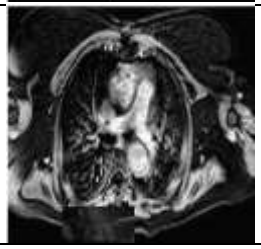	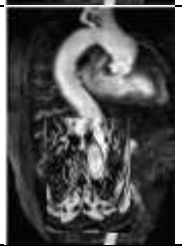	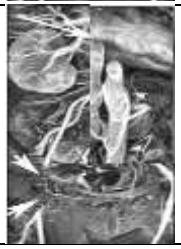		

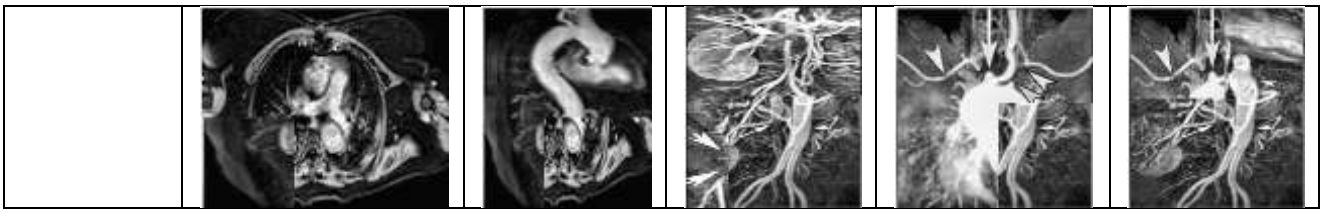

Figure 7 Pre-processed and augmented results using Deep Learning Reconstruction Weighted Contrast Enhanced Pre-processing and CutMix

By applying the above pre-processing contrast enhancement is ensured that in turn aids in visualizing prominent features like edema, a key indicator of active arteritis formation. Moreoverwith the restricted TA samples, CutMix augmentation is applied that by focusing on manipulating relevant diseased regions instead of than random patchesgenerates results of localized diseased features instead of global patterns, therefore resulting in better performance in diagnosing conditions like TA. Figure 8 given below shows the extracted results using Gated Attention-based Deep Multiple Instance Learning.

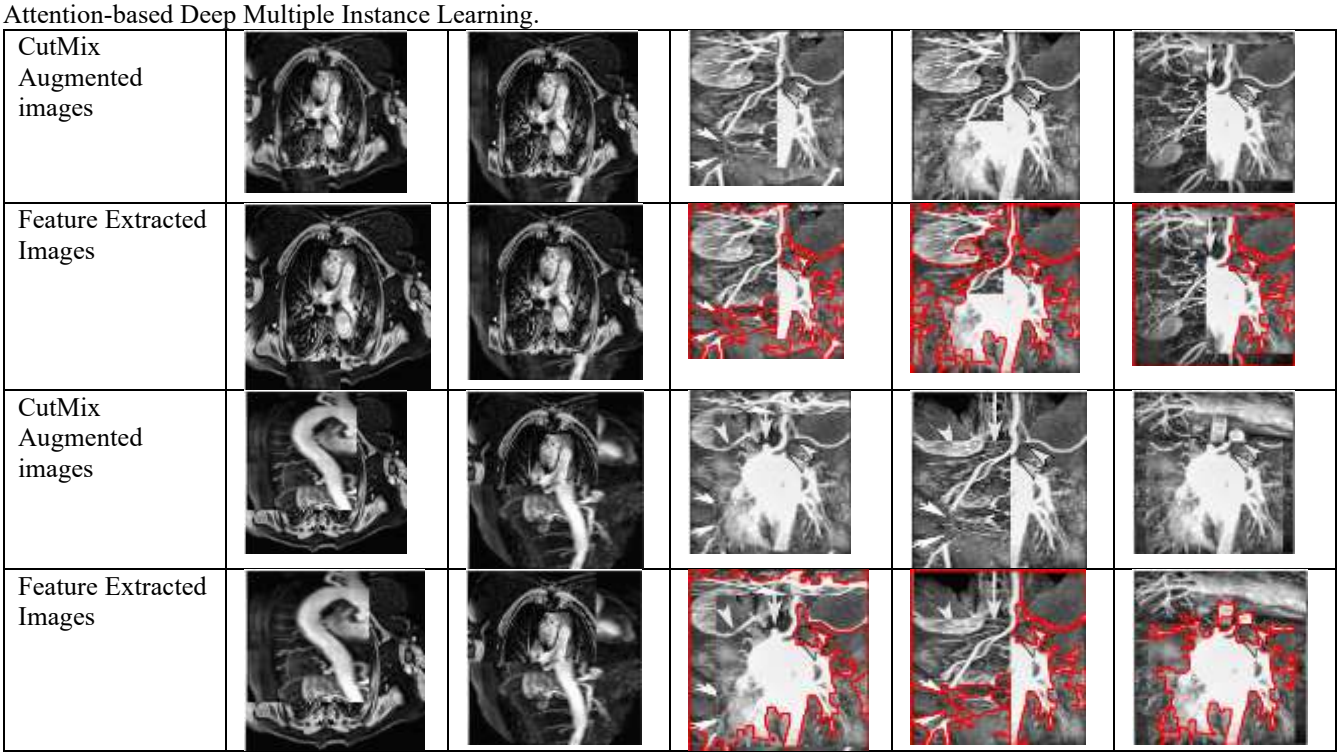

Figure 8 Prominent feature extracted results

As shown in the above figure with the prominent feature extracted results using Discrete Instance Learning and applying ResNet convolved feature extractor in turn extract deep features and finally produce feature map results to bag-level classifier for obtaining classified results. Figure 9 shows the bag-level classifier results.

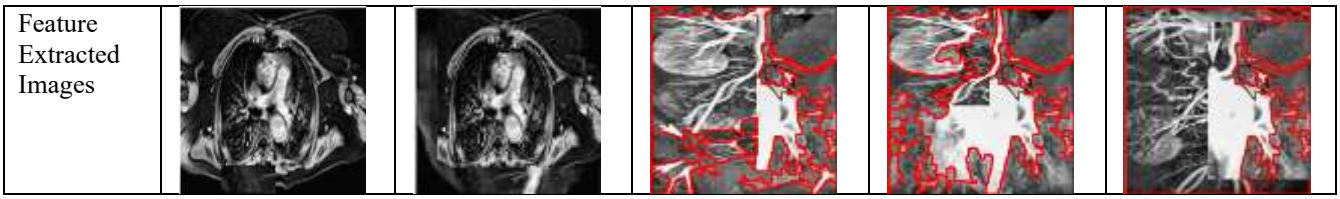

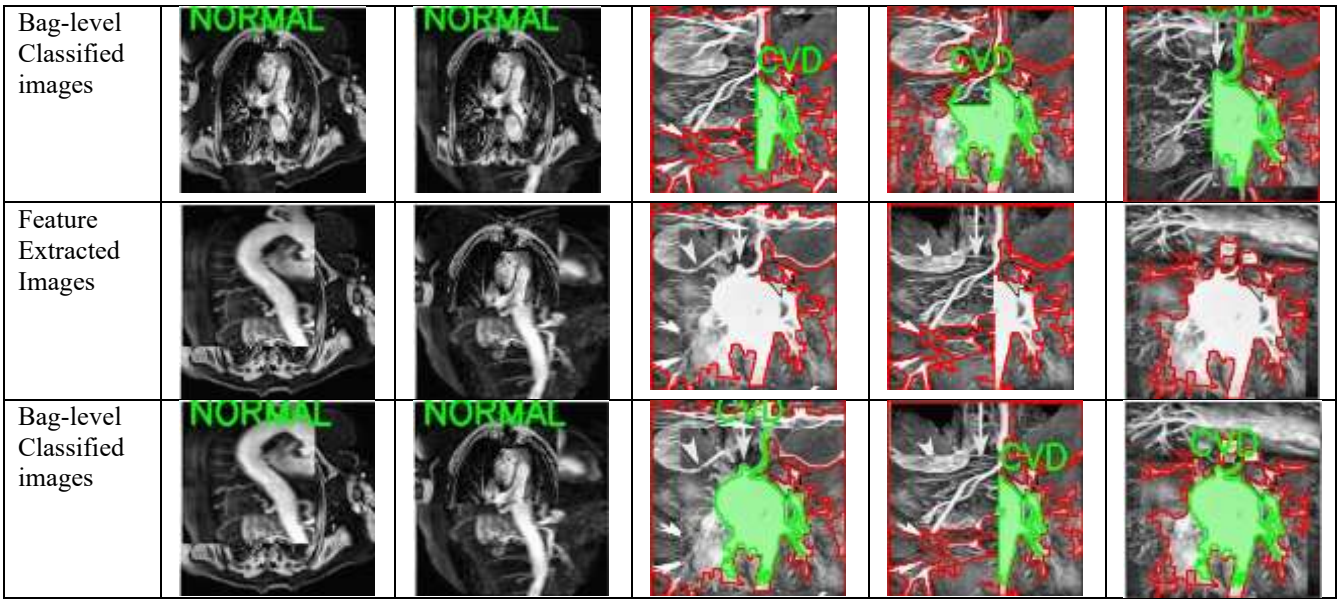

Figure 9 Bag-level classifier results

Also analysis was made with the clinical data consisting of an overall 216 feature to name a few being, observation, age, age at diagnosis, time from onset to diagnosis, gender, race and so on including 57 records. Here missing values were handled along with label encoding in order to maintain uniformity. This is because certain records like gender, checked/unchecked if used as it is results in erroneous data. Hence, before pre-processing the clinical data size was found to be 119.26KB and once performed with pre-processing was found to be 33.43KB. Figure 10 given below shows the pre-processed results of the corresponding clinical data used for analysis.

	Obs	Age	Age at diagnosis	Time from onset to diagnosis (months)	Gender	Race	Seen at Mayo Rochester>	Other Rheum contition	Family Hx of Vasculitis	Family history of Takayasu	Family Hx Other Rheum condition	Hypertensio
0	1	48	39	120.000000	0	3	0	0	0	0	0	
1	2	46	20	24.000000	0	2	1	0	0	0	0	
2	3	43	20	24.000000	0	2	0	0	0	0	0	
3	4	65	29	24.000000	0	2	0	1	0	0	0	
4	5	72	26	24.000000	0	1	0	0	0	0	0	
5	6	53	46	36.000000	0	2	0	0	0	0	0	
6	7	71	26	24.000000	0	2	0	0	0	0	0	
7	8	54	35	48.000000	1	2	0	0	0	0	0	
8	9	30	28	30.000000	0	2	0	1	0	0	1	
9	10	41	27	1.000000	0	2	0	0	0	0	0	

```
Input data shape
(10,216)

Input File Size: 119.26 KB

===== LABEL ENCODING SUMMARY =====
Yes/No Mapping → {'No': 0, 'Yes': 1}
Gender Mapping → {'Female': 0, 'Male': 1}
Checked/Unchecked Mapping → {'Checked': 0, 'Unchecked': 1}


Pre-processed data shape
(10,216)

Pre-processed File Size: 33.43 KB
```

Figure 10 Clinical data pre-processed results

With the pre-processed results for the above clinical data, relevant features for classification L1-regularized Logistic Regression function was applied that automatic performs feature selection process by identifying key predictors for classification. Figure 11 shows the features selected results.

```
===== ALL FEATURES IMPORTANT RANKING =====
```

	Rank	Feature	Coefficient
0	1	Race	0.472614
1	2	Treatment (choice=Cyclophosphamide)	0.451579
2	3	Age	-0.441833
3	4	Follow up?	0.430571
4	5	Stenosis localization (choice=Cervical/Carotids/Vertebral)	0.397430
5	6	Last treatment patient is on (choice=Mycophenolate mofetil)	0.386494
6	7	Treatment (choice=Mycophenolate mofetil)	0.383715
7	8	Arteritis localization (choice=Cervical/Carotids/Vertebral)	-0.378284
8	9	Last treatment patient is on (choice=None)	0.349197
9	10	Pathology results (choice=Carotid)	-0.342093
10	...	...	...
11	207	Vascular intervention performed (choice=Carotid endarterectomy)	0.000000
12	208	Last treatment patient is on (choice=Cyclophosphamide)	0.000000
13	209	Pathology results (choice=Femoral)	0.000000
14	210	Pathology results (choice=Innominate)	0.000000
15	211	Pathology results (choice=Vertebral)	0.000000
16	212	Pathology results (choice=Temporal)	0.000000
17	213	Pathology findings (choice=Other)	0.000000
18	214	Pathology findings (choice=Discordance)	0.000000
19	215	Complications (choice=Mesenteric infarction)	0.000000
20	216	Complete?	0.000000

```
SELECTED FEATURES:

['Age', 'Hypertension', 'Hyperlipidemia at diagnosis', 'Smoker', 'Smoking Hx', 'Gender', 'Symptoms (choice=Fatigue)', 'Symptoms (choice=Malaise)', 'Symptoms (choice=weight loss >5kg)', 'Symptoms (choice=SOB)']
```

Figure 11 L1-regularized Logistic Regression feature selected results

As shown in the above figure prior to feature selection function an overall of 216 features were found, however, post feature selection process prominent 10 features were selected. With the prominent 10 features selected, classification was performed to report the diagnosed results. Figure 12 shows the SVM-based classified results.

	Age	Hypertension	Hyperlipidemia at diagnosis	Smoker	Smoking Hx	Gender	Symptoms (choice=Fatigue)	Symptoms (choice=Malaise)	Symptoms (choice=weight loss >5kg)	Symptoms (choice=SOB)	Diagnosed a Mayo c evaluated withi 1y of D
0	48	1	1	0	0	0	1	1	1	0	
1	46	1	0	0	0	0	1	0	1	0	
2	43	1	1	0	0	0	1	1	1	1	
3	65	1	1	0	0	0	1	1	0	1	
4	72	0	1	1	2	0	1	1	1	1	
5	53	1	0	0	0	0	0	0	1	1	
6	71	1	1	0	0	0	1	1	1	1	
7	54	1	0	1	2	1	0	0	1	1	
8	30	0	0	0	0	0	0	0	0	1	
9	41	1	0	0	1	0	1	1	1	1	

Figure 12 SVM-based classified diagnosed results

As shown in the above figure, age along with factors like, hypertension, hypertension at diagnosis, smoker, smoking Hx, symptoms like fatigue, malaise, weight loss greater than 5kg, shortness of breath plays the major role in determining the diagnosed results.

Case 1: Records 2nd and 6th: From the above results though four symptoms were found to be 1 along with hypertension, hypertension at diagnosis for the corresponding second and sixth record, however, age in case of second record was observed to be 43 whereas in case of the sixth record it was observed to be 71. Hence, here age plays major role in generating the diagnosed results with 2nd record diagnosed result to be 1 whereas the diagnosed results with 6th record diagnosed result to be 0.

Case 2: Records 2nd and 4th: From the above results though four symptoms were found to be 1 along with hypertension at diagnosis to be 1 for the corresponding second and fourth record, however, hypertension was observed to be 0 in case of 4th record. Hence, here hypertension plays major role in generating the diagnosed results with 2nd record diagnosed result to be 1 whereas the diagnosed results with 4th record diagnosed result to be 0.

5. Performance comparison

5.1 Performance analysis of precision, recall and accuracy using images

Precision, recall and accuracy using training images is evaluated based on the true positive rate 'TP' (i.e. normal samples detected as normal), false positive rate 'FP' (i.e. normal samples detected as diseased), true negative rate 'TN' (diseased samples detected as diseased) and false negative rate 'FN' (i.e. diseased samples detected as normal) respectively. Precision is the ratio of the method's positive classifications that are actually positive. Precision is mathematically defined as given below.

$$Pre = \frac{TP}{TP+FP} \tag{12}$$

In the evaluation of cardiovascular risk is patient with TA, precision measures the ratio of normal patients classified as diseased that were actually normal. A hypothetical perfect method is said to generate results with zero false positives and hence a precision of closer of 1.0 observes efficient evaluation. Recall on the other hand is the ratio of all actual normal patients was classified correctly as normal patient.

$$Rec = \frac{TP}{TP+FN} \tag{13}$$

From the above equation false negatives are said to be actual positives or actual normal patients that were misclassified as negatives or diseased patients that is why they appear in the denominator. In the evaluation of cardiovascular risk is patient with TA, recall measures the ratio of normal patients that were correctly classified as normal. Accuracy is the ratio of all classifications that were correct and is mathematically defined as given below.

$$Acc = \frac{TP+TN}{TP+FP+TN+FN} \tag{14}$$

In the evaluation of cardiovascular risk is patient with TA example, accuracy evaluates the ratio of all training images correctly classified.A perfect method would have zero false positives and zero false negatives and hence an accuracy of 1.0, or 100%. Table 2 presents the overall precision, recall and accuracy results for the obtained deep

features using proposed GA-BLC method and also with the other two existing methods, DLR-DB) [1] and eXtreme Gradient Boosting (XGBoost) [2] separately for sample images.

Table 2Tabulation of precision, recall and accuracy for sample images

Samples	Precision			Recall			Accuracy		
	GA-BLC	DLR-DB [1]	XGBoost [2]	GA-BLC	DLR-DB [1]	XGBoost [2]	GA-BLC	DLR-DB [1]	XGBoost [2]
50	0.9	0.85	0.82	0.92	0.89	0.86	0.86	0.8	0.76
100	0.88	0.78	0.73	0.9	0.78	0.75	0.82	0.75	0.7
150	0.87	0.77	0.72	0.87	0.75	0.7	0.8	0.73	0.68
200	0.83	0.73	0.68	0.85	0.73	0.68	0.75	0.68	0.63
250	0.81	0.71	0.66	0.83	0.71	0.66	0.73	0.67	0.62
300	0.79	0.69	0.64	0.81	0.69	0.64	0.71	0.65	0.6
350	0.77	0.67	0.62	0.79	0.71	0.66	0.7	0.62	0.57
400	0.8	0.7	0.65	0.82	0.73	0.68	0.74	0.67	0.62
450	0.83	0.73	0.68	0.85	0.75	0.7	0.79	0.71	0.66
500	0.85	0.75	0.7	0.88	0.8	0.75	0.83	0.75	0.7

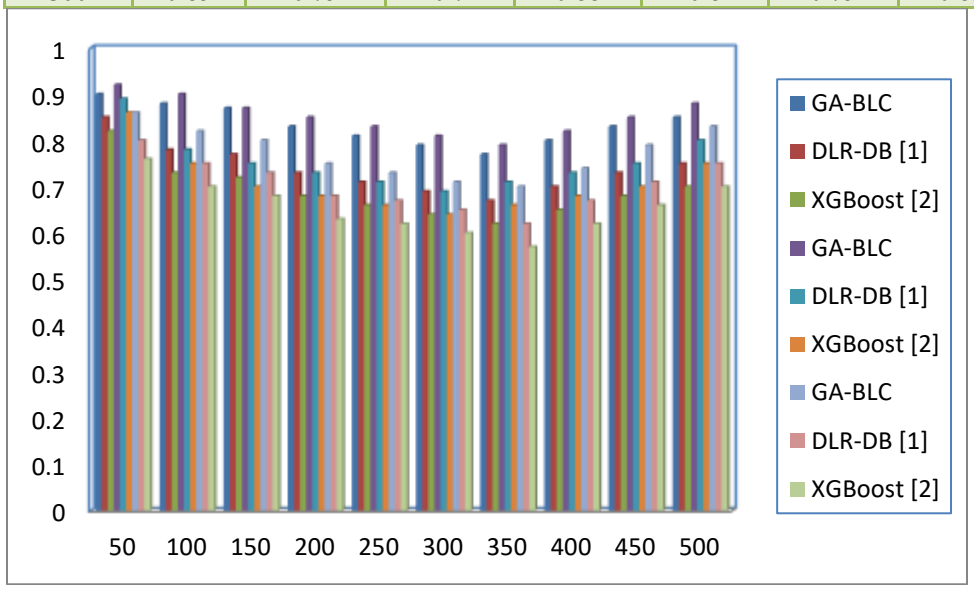

Figure 13 Comparison of precision, recall and accuracy using GA-BLC**, DLR-DB [1] and XGBoost [2] for image [30] [changes made]**

Figure 13 given above illustrate the precision, recall and accuracy results using three methods, GA-BLC, DLR-DB [1] and XGBoost [2] for image [30]. In order to ensure fair comparisons, similar sample from same image is used and result is analyzed. The results from above graph show better precision results using proposed GA-BLC IL method compared to [1] and [2]. To obtain the recall rate results, true positive and false negative values using the three methods were validated and analyzed and substituted in the equation (13). In addition to the values of true positive and false negative, true negative and false positive results are measured and values were substituting in equation (14) to generate accuracy results.The precision improvement using proposed GA-BLC method was owing to the application Gated Attention-based Deep Multiple Instance Learning extractor. Here, by applying this extractor, focuses on relevant instances by selectively filtering information in medical imaging to obtain the key clinical predictors and also key MRA findings. Following which gated attention mechanisms was employed to learn the instances within a bag that are found to be the most important. This in turn selected the features that were strongly associated to the target variable, therefore improving precision using proposed GA-BLC method by 11% compared to [1] and 17% compared to [2] along with improving overall recall using proposed GA-BLC method by 12% compared to [1] and 17% compared to [2]. Third the accuracy improvement using proposed GA-BLC method was due to the application of bag-level classifier for measuring cardiovascular disease risk in TA patients. By applying this classifier with multiple instance

learning classifies patients based on the overall bag pattern than depending of simple scoring mechanism. Owing to this precise and accurate differentiation between classes (i.e. diseased and normal) is made in a significant manner. This in turn improves overall accuracy of proposed GA-BLC method by 8% compared to [1] and 15% compared to [2].

5.2 Performance analysis of false positive rate using images

The false positive rate (FPR) is the ratio of all actual negatives or diseased samples that were classified incorrectly as positives or normal samples. The false positive rate is also known as the probability of false alarm**.** The FPR is mathematically defined as given below.

$$FPR = \frac{FP}{FP+TN} \quad (15)$$

From the above equation (15) the false positives are actual negatives that were misclassified and hence are represented in the denominator. In the evaluation of cardiovascular risk is patient with TA, FPR measures the ratio of normal training images that were incorrectly classified as diseased image. Table 3presents overall false positive rate results of sample images for proposed GA-BLC method, two existing methods, DLR-DB) [1] and eXtreme Gradient Boosting (XGBoost) [2].

Table 3Tabulation of false positive rate for sample images

Samples	False positive rate		
	GA-BLC	DLR-DB [1]	XGBoost [2]
50	0.36	0.5	0.58
100	0.3	0.4	0.45
150	0.45	0.55	0.6
200	0.49	0.59	0.64
250	0.52	0.62	0.67
300	0.57	0.57	0.62
350	0.51	0.61	0.66
400	0.47	0.57	0.62
450	0.41	0.51	0.56
500	0.38	0.48	0.53

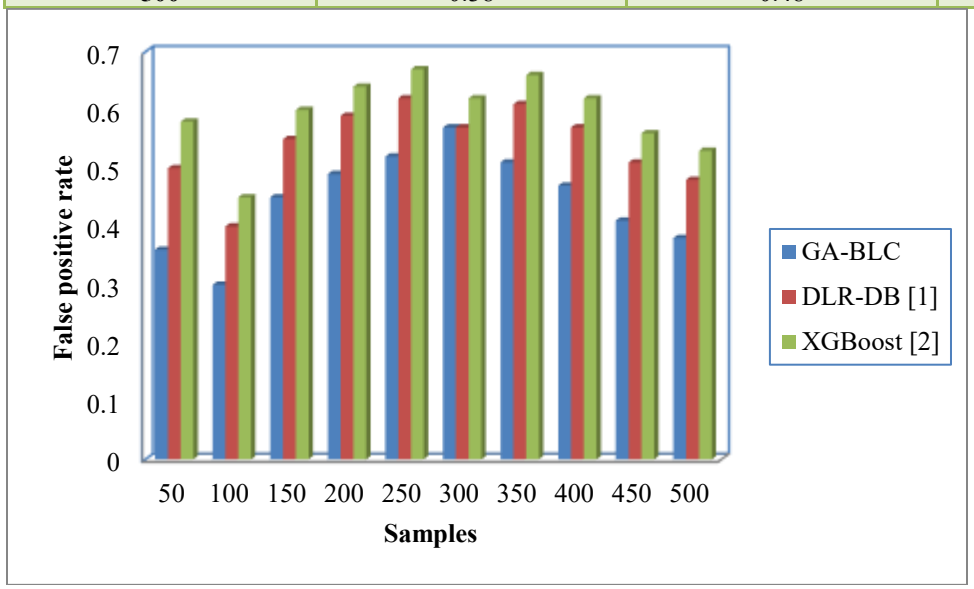

Figure 14 Comparison of false positive rate using GA-BLC**, (DLR-DB) [1] and XGBoost [2] for image [30][changes made]**

Figure 14 illustrates the false positive rate using the three methods GA-BLC, (DLR-DB) [1] and XGBoost [2] for image [30] for image samples ranging between 50 and 500 performed over a simulation of ten runs. From the above figure for the first six iterations, the false positive rate tends to be increasing with the increased in the samples for the

three methods. However, for the remaining four iterations a rise in false positive rate was found therefore corroborating the objective that increase in or decrease in samples does not affect the results. The reason was by applying the Multiple Instance Learning employed with multiple instance learning to learn from unstructured data like entire slide images by taking into consideration the patches as instances within a bag, therefore reducing the false positive rate of GA-BLC method by 23% compared to [1] and 35% compared to [2].

5.3 Performance analysis of false negative rate using images

Finally the false negative rate is evaluated as the ratio of positive or diseased samples that are incorrectly identified as negative of normal samples. This is mathematically defined as given below.

$$FNR = \frac{FN}{FN+TP} \quad (16)$$

Table 4presents the false negative rate results for 500 distinct samples images using GA-BLC, DLR-DB [1] and XGBoost [2].

Table 4 Tabulation of false negative rate for sample images

Samples	False negative rate		
	GA-BLC	DLR-DB [1]	XGBoost [2]
50	0.07	0.1	0.13
100	0.11	0.17	0.21
150	0.15	0.21	0.25
200	0.19	0.25	0.29
250	0.22	0.28	0.32
300	0.25	0.31	0.35
350	0.27	0.33	0.27
400	0.23	0.29	0.34
450	0.19	0.25	0.29
500	0.15	0.21	0.25

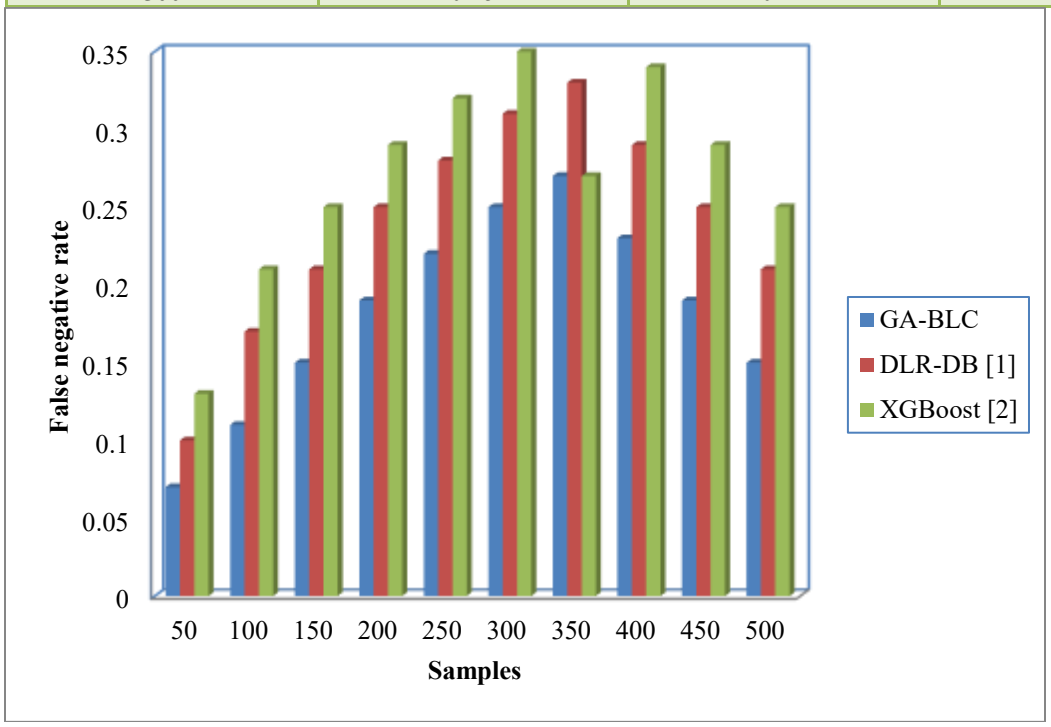

Figure 15 Comparison of false negative rate using GA-BLC**, (DLR-DB) [1] and XGBoost [2] for sample image [changes made]**

Figure 15 shows the graphical presentation of false negative rate using GA-BLC, (DLR-DB) [1] and XGBoost [2] for sample image provided as input ranging between 50 and 500. To ensure fair comparison similar amount and sample

images were given as input and simulations were performed using the three methods. With simulations performed for 50 images the false negative rate using the three methods were observed to be 3, 4 and 5 with the true positive being 36, 34 and 33 respectively for the three methods. By substituting the values in equation (16) the results were observed to be 0.07, 0.10 and 0.13, confirming the improvement in terms of false negative rate for the proposed GA-BLC. The reason was by applying the ResNet Convolved Feature Extractor model extracts deep features, following which the activation function works on the convoluted results to generate feature map results. Finally with the aid of fully connected layer results of the features being extracted fed to the bag-level classifier for classification task. This in turn reduces the false negative rate of proposed GA-BLC method by 34% compared to [1] and 55% compared to [2].

5.4 Performance analysis of precision, recall, accuracy, positive rate and false negative rate using clinical data

In this section the performance analysis of five different performance metrics to analyze the cardiovascular risk in patients in TA using clinical data is provided in table 5.

Table 5Tabulation of precision, recall, accuracy, false positive rate and false negative rate for clinical data

Methods	Precision	Recall	Accuracy	False positive rate	False negative rate
GA-BLC	0.95	0.94	0.97	0.05	0.07
DLR-DB [1]	0.89	0.9	0.91	0.055	0.075
XGBoost [2]	0.82	0.85	0.85	0.063	0.082

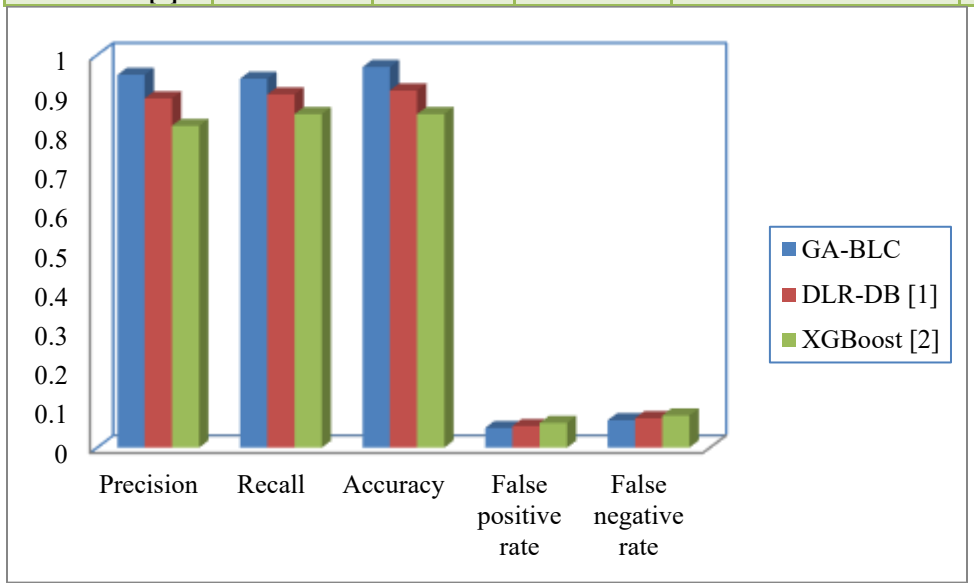

Figure 16 Comparison of precision, recall, accuracy, false positive rate and false negative rate using GA-BLC, **(DLR-DB) [1] and XGBoost [2] for clinical data [28] [changes made]**

Finally figure 16 given above shows the results of five different performance metrics, precision, recall, accuracy, false positive rate and false negative rate for three different methods, GA-BLC, (DLR-DB) [1] and XGBoost [2] when substituted with clinical data for analysis. From the above figure, an overall analysis for 57 samples were made and the average values recorded by substituting the values in equations (12) to (16). From the above figure the precision, recall and accuracy of the GA-BLC method was found to be comparatively better than [1] and [2]. The reason was missing values were handled and to ensure uniformity label encoded results were generated for yes/no mapping, gender mapping and checked/unchecked samples. Moreover to the pre-processed samples logistic regression function was applied to the overall features with the intent of selecting prominent features present in the dataset. By applying the logistic regression function for the samples and features in clinical data discarded irrelevant features. With this the overall precision was improved by 6%, 8% with improvement in recall observed to be 4%, 6% and accuracy improvement found to be 6% and 7% compared to [1] and [2]. Also by applying the pre-processed samples along with the relevant features selected results to SVM based classifier accurately detected classified results. With this the overall false positive rate was found to be reduced using GA-BLC method by 10% compared to [1] and 15% compared to [2] respectively.

5.5 Inter-rater and Intra-rater Reliability

Inter-rater and intra-rater reliability in TA is primarily measured to assess disease activity and damage. In our work the performance metrics, inter-rater and intra-rater reliability formulas interpolate consistency, using Cohen's Kappa methods. This is mathematically denoted as given below.

$$\kappa = \frac{Prop_{OA} - Prop_{CA}}{1 - Prop_{CA}} \quad (17)$$

From the above equation (17) the inter-rater and intra-rater reliability is measured via Cohen's Kappa coefficient 'κ' with the aid of proportion of observed agreement '$Prop_{OA}$' and proportion of chance agreement '$Prop_{CA}$' respectively.

Table 6 Tabulation of inter-rater reliability and intra-rater reliability

Methods	Inter-rater reliability	Intra-rater reliability
GA-BLC	0.75	0.77
DLR-DB [1]	0.69	0.70
XGBoost [2]	0.65	0.65

The table given above lists the values of inter-rater and intra-rater reliability using the proposed GA-BLC and two existing methods, DLR-DB [1] and XGBoost [2] respectively. As far as imaging is concerned, the mean Cohen's Kappa ranges between 0.72 and 0.79 referring to the good reliability measure. As given in the above table the inter-rater and intra-rater reliability of the proposed GA-BLC method was found to be better than [1] and [2]. In the proposed method GA-BLC by employing Gated Attention-based Deep Multiple Instance Learning extractor thatin turn learns from entire slide images by taking into consideration the patches as instances within a bag therefore reduces false positive and false negative rate. With this the overall inter-reliability and intra-reliability of the GA-BLC method was found to be better by 8% compared to [1] and 6% compared to [2] respectively.

5.6 Discussion and limitations

This work proposes a Gated Attention Deep Multiple Instance Learning (GA-DMIL) for analyzing cardiovascular risk in patients with TA. The proposed GA-DMIL method incorporated
pre-processing, augmentation along with deep learning with the objective of identifying cardiovascular Prediction in Patients with Takayasu Arteristis. The GA-DMIL method surpassed other existing methods in terms of precision by 14%, recall by 15% and accuracy by 12%. Moreover it manifested better performance results while identifying cardiovascular Prediction in Patients with Takayasu Arteristis with minimal false positive by 24% and false negative by 44% compared to DLR-DB [1] and XGBoost [2]. In spite of its advantages observed in terms of different performance metrics, however early diagnosis i.e., before stenosis or aneurysm occurs were not analyzed therefore compromising the accuracy and true positive rate.

6. Conclusion

Cardiovascular risk in patients with TA is a demanding task owing to its rare nature and chronic inflammatory disease that require long term monitoring and treatment to prevent serious complications. In this paper, we propose the GA-BLC, a Gated Attention Deep Multiple Instance Learning based method for cardiovascular risk in patients with TA. GA-BLC adopts a Deep Learning Reconstruction Weighted Contrast Enhanced Pre-processing model with CutMix augmentation to split augmented samples into fixed-size patches, therefore improving sensitivity and accuracy for the detection and assessment compared to traditional methods accuracy. To extract prominent features required for classification, Gated Attention-based Deep Multiple Instance Learning extractor is applied with multiple instances learning to learn from entire slide images by taking into consideration the patches as instances within a bag therefore minimizing false positive and false negative rate extensively. GA-BLC then efficiently uses the bag-level classifier that provides accurate results by analyzing homogeneous subgroups of the disease than depending on simple scoring systems. Experiments on the clinical TA dataset and MRA images show that the GA-BLC method outperforms all baselines in terms of precision, recall, accuracy, false positive rate, false negative rate, inter-reliability and intra-reliability.

In conclusion, the findings of the present study demonstrated TA using MRA images. However early stage identification in TA using MRA may be difficult to determine. Further study using MRI techniques is necessary to detect the disease activity in Takayasu arteritis at an early stage with improved accuracy and true positive rate. Future work would focus on the application of Magnetic Resonance Images (MRI) for early (i.e. pre-pulseless) stage detection by identifying structural wall changes prior to occurrence of severe stenosis.

References

[1] Ning Ding, Xi-Ao Yang, Min Xu, Yun Wang, ZhengyuJin, Yining Wang, HuadanXue, Lingyan Kong, Zhiwei Wang, Daming Zhang, "Large vessel vasculitis evaluation by CTA: impact of deep-learning reconstruction and "dark blood" technique", Insights into imaging, Springer, Jul 2024 [Deep Learning Reconstruction with Dark Blood (DLR-DB)]

[2] Yi-Ting Lu, Zeng-Lei Zhang, Xing-Yu Zhou, Di Zhang, Tao Tian, Peng Fan, Ying Zhang, Xian-Liang Zhou, "Predicting stroke and myocardial infarction risk in Takayasu arteritis with automated machine learning models", iScience, Elsevier, Vol. 26, Dec 2023 [eXtreme Gradient Boosting (XGBoost)]

[3] Lourdes Ortiz-Fernandez, GuherSaruhan-Direskeneli, Fatma Alibaz-Oner, SemaKaymaz-Tahra,, "Identification of susceptibility loci for Takayasu arteritis through a large multi-ancestral genome-wide association study", American Society of Human Genetics, Jan 2021

[4] Berit D. Nielsen, Luca Seitz, Wolfgang A. Schmidt, "Update in imaging for large vessel vasculitis", Best Practice & Research Clinical Rheumatology, Elsevier, Vol. 39, Sep 2025

[5] Xianghu Yan, Lingping Ran, Lixian Zou, Yi Luo, Zhaoxia Yang, Shiyu Zhang, Shuheng Zhang, Jian Xu, Lu Huang, Liming Xia, "Dark blood T2-weighted imaging of the human heart with AI-assisted compressed sensing: a patient cohort study", Quantitative Imaging in Medicine and Surgery, Jun 2022

[6] Luuk J. Oostveen, Frederick J. A. Meijer, Frank de Lange, Ewoud J. Smit, Sjoert A. Pegge, Stefan C. A. Steens, Martin J. van Amerongen, Mathias Prokop, IoannisSechopoulos, "Deep learning–based reconstruction may improve non-contrast cerebral CT imaging compared to other current reconstruction algorithms", Springer Nature Link, Vol. 31, Mar 2021

[7] Feyyaz Hazar Yagmur, MuhammetEmin Kutu, FatihTastekin, AysegulAvcu, Senar S¸ TugbaOcak, FatihYıldırım, Hasan Kocaayan,SafiyeBakkal, SemaIsık, "Long term outcomes of aortic valve insufficiency in patients with takayasuarteristis", Frontiers in Immunology, Sep 2025

[8] Tong Su, Zhe Zhang, Yu Chen, Yun Wang, Yumei Li, Min Xu, Jian Wang, Jing Li, Xinping Tian, ZhengyuJin, "Dark-Blood Computed Tomography Angiography Combined With Deep Learning Reconstruction for Cervical Artery Wall Imaging in Takayasu Arteritis", Neuroimaging and Head & Neck, Feb 2024

[9] Jihang Sun, Haoyan Li, Jianying Li, HaiyunLi , Michelle Li, Zuofu Zhou, "Application of Deep Learning Image Reconstruction (DLIR) Algorithm to Improve Image Quality in CT Angiography of Children with Takayasu Arteritis", Nov 2021

[10] Mena Samaan, Arevik Abramyan, Srihari Sundararajan, Emad Nourollah-Zadeh, Hai Sun, Anil Nanda, Sudipta Roychowdhury, Gaurav Gupta, "Cerebrovascular implications of takayasu arteritis: a review", Neuroradiology, National Library of Medicine, Oct 2024

[11] Nikolaos Taprantzis, Dimosthenis Chrysikos, Amir Shihada, Theodore Troupis, "Prevalence and clinical severity of takayasu arteritis angiographic types: a systematic review with meta-analysis", Rheumatology International, Springer Nature Link, Vol. 45, Sep 2025

[12] David Saadoun, Alessandra Bura-Riviere, ChloéComarmond, Marc Lambert, Alban Redheuil, Tristan Mirault, "French recommendations for the management of Takayasu's arteritis", Orphanet Journal of Rare Diseases", Springer Nature Link, Vol. 16, Jul 2021

[13] Chiara Marvisi, ErtugrulCagriBolek, Mark A. Ahlman, Hugh Alessi, Christopher Redmond, Francesco Muratore, Elena Galli, Caterina Ricordi, SemaKaymaz-Tahra, Salih Ozguven, Fatma AlibazOner, HanerDireskeneli, Carlo Salvarani, Kaitlin A. Quinn, Peter C. Grayson, "Development of the Takayasu's Arteritis Integrated Disease Activity Index", Arthritis Care & Research, Wiley, Apr 2024

[14] Franco Dammacco, Anna Cirulli, Annalisa Simeone, Patrizia Leone, Raffaele Pulli, Domenico Angiletta, Giuseppe Rubini, Alessandra Di Palo, Angelo Vacca, Rosanna Dammacco, "Takayasu arteritis: a cohort of Italian patients and recent pathogenetic and therapeutic advances", Clinical and Experimental Medicine, Springer, Jan 2021

[15] Min Liu, Weifang Liu, Haoyuan Li, Xiaoming Shu, Xincao Tao, ZhenguoZhai,, "Evaluation of takayasu arteritis with delayed contrast-enhanced MR imaging by a free-breathing 3D IR turbo FLASH", Medicine, Nov 2017

[16] Xiaojuan Guo, Min Liu, Mingxi Liu, Zhanhong Ma, Juanni Gong, Yuanhua Yang, Wei Gao, Jiaoyan Wu, Qi Yang, Min-Fu Yang, "Delayed contrast-enhanced magnetic resonance imaging enables detection of pulmonary artery lesions in Takayasu's arteritis", Quantitative Imaging in Medicine and Surgery", Oct 2023

[17] Marı´a Elena Soto, Gabriela Meléndez-Ramı´rez, Aloha Meave-Gonzalez, Stephan Achenbach, Eid-LidtGuering, Erick Alexa´nderson-Rosas, "Coronary CT Angiography in Takayasu Arteritis", JACC, Cardiovascular Imaging, Vol. 4, Oct 2011

[18] Ayaz Aghayev, Brittany Weber, Tiago Lins de Carvalho, Andor W.J.M. Glaudemans, Pieter H. Nienhuis, Kornelis S.M. van der Geest, Riemer H.J.A. Slart, “Multimodality imaging to assess diagnosis and evaluate complications of large vessel arteritis”, Journal of Nuclear Cardiology, Elsevier, Vol. 37, Jul 2024
[19] F P Zhu, 1s Luo, Z J Wang, Z Y Jin, L J Zhang, G M Lu,, “Takayasu arteritis: imaging spectrum at multidetector CT angiography”, The British Journal of Radiology, Oct 2012
[20] Guillaume Goudot, Anatole Jimene, Nassim Mohamed, Jonas Sitruk, Lina Khider, Hélène Mortelette, Clément Papadacci, Fabien Hyafi, Micka¨elTanter, Emmanuel Messas, Mathieu Pernot, Tristan Mirault, “Assessment of Takayasu’s arteritis activity by ultrasound localization microscopy”, Archives of Cardiovascular Diseases Supplements, Elsevier, Vol. 15, Jan 2023
[21] Loris Azoyan, Matthieu Bonjour, Olivier Steichen, “Diagnostic Accuracy of Clinical Findings for Takayasu Arteritis: A Rapid Review and Meta-Analysis”, International Journal of Vascular Medicine, Wiley, Aug 2025
[22] Kazumasa Oura,MaoYamaguchiOura,RyoItabashi, TetsuyaMaeda, “Vascular Imaging Techniques to Diagnose and Monitor Patients with Takayasu Arteritis: A Review of the Literature”, Diagnostics, MDPI, Oct 2021
[23] Siyuan Chen, Xiao Cui, Yue Chen, Xiaogang Guo, “Biologic therapies for the treatment of large vessel vasculitis: A systematic review and meta-analysis”, PLOS ONE, Mar 2025
[24] H.S. Natraj Setty, J.R. Vijaykumar, C.M Nagesh, Shivanand S Patil, Santhosh Jadav, T.R. Raghu, C.N. Manjunath, “Takayasu’s arteritis - a comprehensive review”, Journal of Rare Diseases Research and Treatment, Mar 2017
[25] Linfeng Xi, Anqi Liu, Han Kang, Yifei Ni, Jianping Wang, Hongyi Wang, Xiaoyan Li, f Xiaojuan Guo, Minjie Lu, Hui Liu, “Developing a deep learning-based imaging diagnostic framework, PVDNet, for differentiating pulmonary artery sarcoma and pulmonary thromboembolism: a multi-center observational study”, The Lancet Regional Health - Western Pacific, Oct 2025
[26] Jason M Tarkin, Christopher Wall, Deepa Gopalan, Luigi Aloj, RoidoManavaki, Tim D Fryer, Eric O Aboagye, Martin R Bennett, James E Peters, James H F Rudd, Justin C Mason, “Novel Approach to Imaging Active Takayasu Arteritis Using Somatostatin Receptor Positron Emission Tomography/Magnetic Resonance Imaging”, Circulation Cardiovascular Imaging, Jun 2020
[27] Carolina Bezzi, Alessandro Tomelleri, Sara Resta, Federico Fallanca, CampochiaroCorrado, Elena Baldissera, SamueleGhezzo, Nicola Farina, Lorenzo Dagna, Arturo Chiti, Paola Mapelli and Maria Picchio, “Predicting one-year Takayasu Arteritis Relapse using [18F]FDG PET and Convolutional Neural Networks”, The Journal of Nuclear Medicine, Jun 2025
[28] https://data.mendeley.com/datasets/3cfj465shk/1
[29] Pedro Manuel Oliveira, Paula Fereira, Fabio Murteira, Ines RueffRato, Marta Barbedo, “ Takayasu Arteritis as a Secondary Cause of Arterial Hypertension”, International Journal of Cardiovascular Sciences, Jul 2021
[30] Michael B. Gotway, Philip A. Araoz, Thanila A. Macedo, Anthony W. Stanson, Charles B. Higgins, Ernest J. Ring, Samuel K. Dawn, W. Richard Webb, Jessica W. T. Leung, Gautham P. Reddy, “Imaging Findings in Takayasu’s Arteritis”, American Journal of Roentgenology, Vol. 184, Nov 2012